EXPERIMENTAL ANALYSIS OF LOW-RANK COAL COMBUSTION UNDER AIR AND OXY-FUEL CONDITIONS

Adriano Carotenuto, adriano.carotenuto@ufrgs.br
Rodrigo Corrêa da Silva, correada@tu-cottbus.de
René Lúcio Rech[a], renerech@gmail.com
Paulo Smith Schneider[a], pss@mecanica.ufrgs.br
Nilson Romeu Marcílio[a], nilson@enq.ufrgs.br
Hans Joachim Krautz[b], krautz@tu-cottbus.de

[a]School of Engineering, Federal University of Rio Grande do Sul, Porto Alegre, Brazil
[b]Chair of Power Plant Technology, Brandenburg University of Technology Cottbus, Germany

Abstract. *An experimental study is performed in a laboratory facility, designed to investigate the combustion process under turbulent and swirling flows and covering a temperature range similar to those found in existing furnaces. The global kinetic parameters are determined with the aid of gas-potentiometric analysis by using oxide-ion conducting solid electrolytes. The complete samples burn-out sieved to a size range of 1.250-2.000 mm is evaluated under air-firing and oxy-fired conditions (21% O_2 and 79% CO_2 in vol.). Oxygen concentrations curves for the combustion process are plotted for both oxidant environments. Tests are performed for 3 levels of gas temperature, keeping the same O_2 concentration at the feeding stream. Results show higher fuel reactivity under oxy-fuel than air-fired conditions. The influence of the swirling flow within the cyclone reactor on the results is commented.*

Keywords*: Oxy-fuel combustion, lignite coal, effective reaction rate constant, gasification reaction*

1. NOMENCLATURE

C	Molar concentration, mol m^{-3}	*Abbreviations*	
f	Molar fraction, -	daf	Dry, ash free
F	Faraday constant, 9.648×10^4 C mol^{-1}	vol.	Volume
k_{eff}	Effective constant reaction rate, $(mol\ m^{-3})^{n-1}\ s^{-1}$	*Subscripts*	
N	Number of moles	0	Initial
n	Order of reaction, -	atm	Atmospheric
$\dot{n}$	Molar flow, mol s^{-1}	cons	Consumed
P	Pressure, atm	eff	Effective
R	Constant of ideal gas, 8.314 J mol^{-1} K^{-1}	el	Electrons of oxygen
r	Reaction rate, mol m^{-3} s^{-1}	gas	Gas oxygen
T	Temperature, K	in	Reactor inlet
t	Time, s	out	Reactor outlet
U	Cell potential, mV	ref	Reference
$\dot{V}$	Volumetric flow, m^3 s^{-1}	th	Thermal
X	Conversion, -	tot	Total

2. INTRODUCTION

Many works have been carried out in the last years in order to understand the influence of the presence of CO_2 on devolatilization and ignition (Toftegaard et al., 2010), and volatile and char burnout (Brix et al., 2010; Zhang et al., 2010). The literature reveals a significant number of works on the impacts of oxy-fuel atmospheres on lignite combustion (Tappe and Krautz, 2009; Zhang et al., 2010b). Additionally, most of these studies were carried out applying standard techniques of analysis, such as thermogravimetric tests (Liu, 2009) and entrained-flow reactors (Rathnam et al., 2009). It is well-known that thermogravimetric tests operate in conditions far from those in real furnaces, whereas entrained flow reactors are the unique equipments that can simulate more closely practical combustion environments. Consequently, there is a need of quantitative information obtained by reactors which operate in conditions encountered in existing furnaces. Successful results have been obtained with fluidized bed reactor to understand the combustion behavior of solid fuels under air-fired conditions with the aid of solid electrolyte oxygen sensor as stabilized zirconia to calculate the global kinetic parameters (Lorentz and Rau, 1998).

In this present work, data are reported for lignite coal based on experimental activities carried out in $20kW_{th}$ experimental facility. This novel laboratory scale test facility utilizes a cyclone reactor for combusting several types of coal. A gas-potentiometric analysis by using oxide-ion conducting solid electrolytes as stabilized zirconia is utilized to measure oxygen concentration within the reactor during the combustion of coal samples. The results obtained are used to calculate the global kinetic parameters by applying the oxygen balance method (Lorentz and Rau, 1998).

Further information on experimental method and mathematical formulation applied in this study are presented in the next sections.

3. DESCRIPTION OF THE LABORATORY FACILITY

A schematic diagram of the experimental setup is shown in Fig. 1. The combustion takes place in a cyclone reactor with a rated capacity of 20 kW_{th}. Basically, crushed and pre-dried coal is previously transported into a storage silo which feeds a metering system. The size of the coal particles for continuous operation should not be smaller than 0.05 mm and should not exceed 2.000 mm. The coal can be also inserted into the reactor discontinuous by means of an independent system for investigation of rates of the combustion process of single samples.

Combustion air is supplied by a fan of variable rotation speed, whereas in the case of oxy-fuel combustion, O_2 and CO_2 are supplied by storage tanks. In this case, the gas flow is controlled with pressure regulators and valves and the flow rate measured using calibrated rotameters. Flow rate upstream of the furnace are also measured with an orifice plate for all operating conditions. To increase the temperature of oxidant stream before entering into the furnace a preheater and a gas-burner operated with propane are installed.

After the reactor, the flue gas is passed through a cyclone dust separator to remove the fly ash and other particulates before being cooled with an air quench and directed to the stack. The pressure within the furnace controlled by an induced draft fan is maintained near the atmospheric pressure. Gaseous samples are collected and conducted to the gas conditioning device, in which electrically heated tubes are maintained at 473 K to avoid water vapor condensation. Thus, all the standard gaseous concentrations, i.e. O_2, CO_2, NO, CO and SO_2 can be measured on a dry basis in gas analyzer. Additionally, the water vapor and O_2 amount in the oxidizer stream are also monitored.

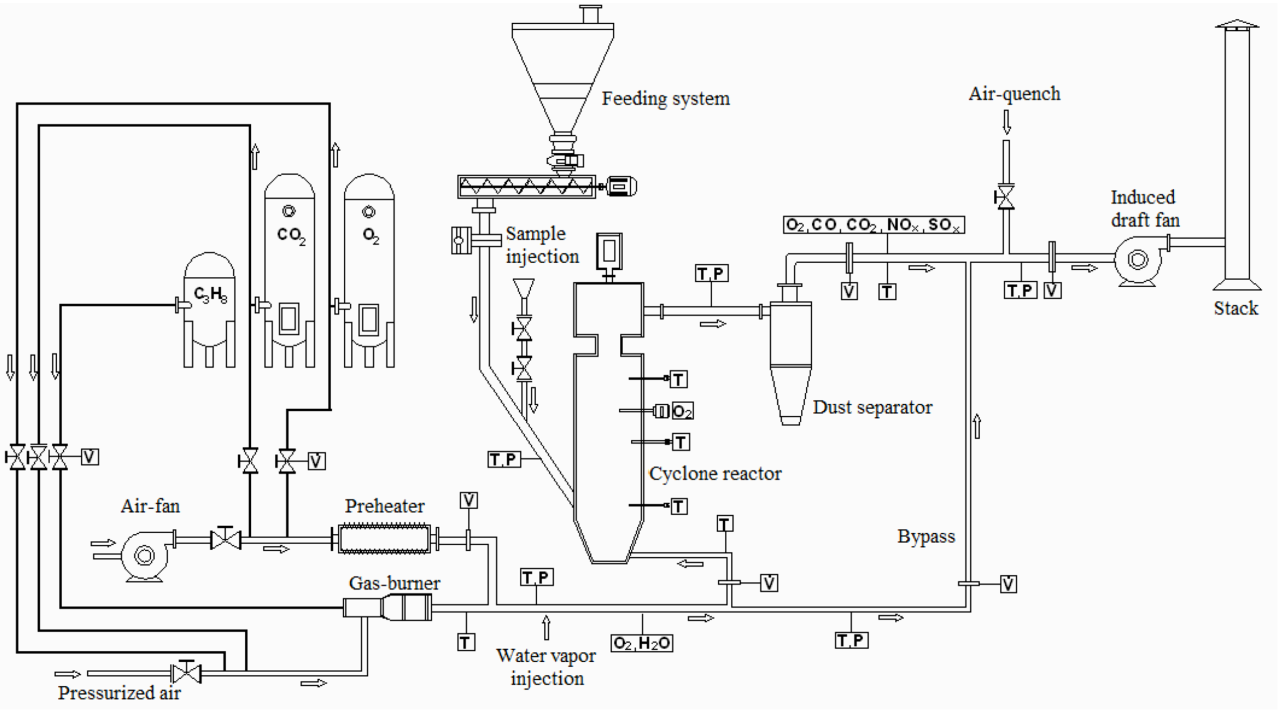

Figure 1. Schematic of the furnace and measurement points (T: temperature, P: pressure and $\dot{V}$: volumetric gas flow).

The combustion chamber illustrated in Fig. 2, is constructed in stainless steel. The oxidizer is injected into the reactor with a temperature around 900 K and can be injected tangentially at four different positions, whereas the coal particles are injected perpendicularly to the wall at 0.170 m distant from the bottom of reactor. The reactor volume where the reaction takes place is 0.0075 m^3. The reactor dimensions are 1.0 m height and 0.140 m internal diameter. Due to its geometry, intensive rotation of the flame within the reactor caused by high velocities, allows a higher burnout while the whirling flames moves upward. The ratio of angular momentum to the axial momentum of the cold flow (swirling number) is approximately between 1.5 and 2.5. The combustion reactor is electrically heated enabling a constant wall temperature up to 1350 K.

Three type-K thermocouples measure the gas temperatures along the inner surface of the reactor and they are positioned, as detailed in Fig. 2b. On the top of the reactor, a simple camera system is utilized to register the image of the combustion. For the investigation of the global kinetic parameters, an oxygen-solid electrolyte sensor is used to acquire the oxygen partial pressure within the combustion chamber.

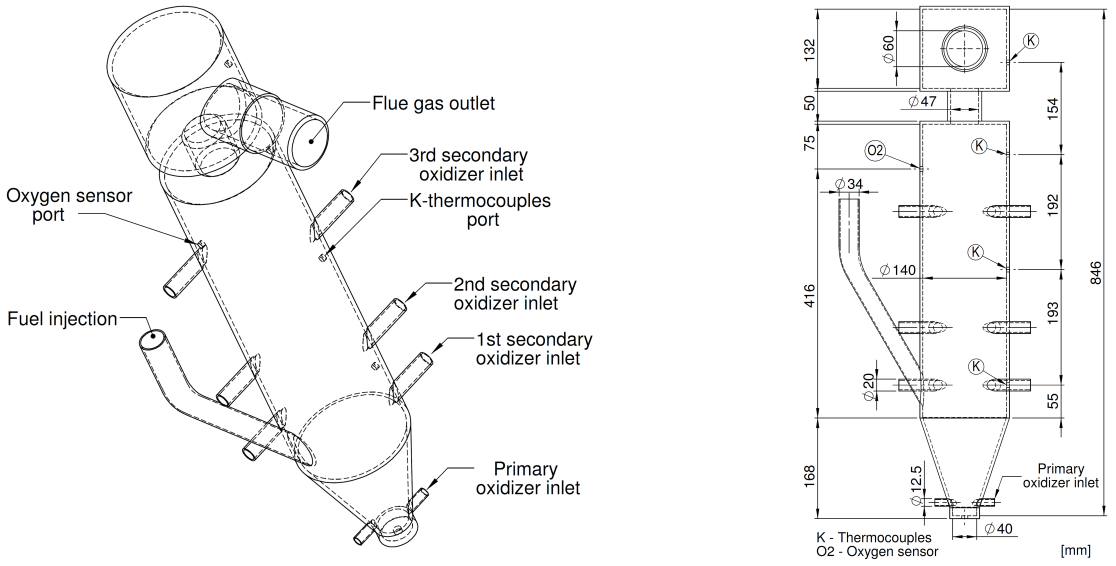

(a) (b)

Figure 2. Perspective (a) and projected (b) views of the cyclone combustion reactor.

4. EXPERIMENTAL APPROACH TO DETERMINE KINETIC PARAMETERS

The test procedure for obtaining the global kinetic parameters from this test facility was extensively studied by (Tappe, 2009). To exemplify how the experiment is performed, the Fig. 3 illustrates the behavior of the oxygen and temperature within the combustion chamber during a trial of a 3-g-sample of lignite under air conditions at 1073 K average temperature. The Fig. 3b is a separated view of the coal sample combustion showed in Fig. 3a, O_2 (vol. %).

Basically, this test facility is continuously fed with coal in order to reach high temperature levels in the reactor to run the experiments with coal samples. When the temperature set in the reactor is reached, the continuous fuel feeding is stopped in order to increase the oxygen concentration within the reactor to the level required to perform the experiments, as for instance, 21% vol. O_2. It's noteworthy to mention that, because the combustion process is interrupted for a while, all three measured points of temperature within the furnace (at bottom, middle and top) decrease and the average of these temperatures determines the experiment combustion gas temperature within the reactor to calculate the kinetic parameters. When new steady conditions are established, i.e. constant temperatures and oxygen concentration are reached, the discontinuous fuel valve is opened and the coal sample is injected into the reactor.

As depicted in Fig. 3b, the starting point of the combustion sequence is characterized by the sudden drop of the oxygen concentration due to the predominance of combustion of volatiles matter right after the injection of the sample, followed by the combustion of the char mass until the oxygen concentration reaches initial concentration. Afterwards, the continuous feed is restarted in order to reach necessary temperature conditions for the next trial. Determination of global kinetic parameters is based on the variation of oxygen concentration measured by oxygen-solid electrolyte sensor and time average temperatures measured by the three thermocouples during the combustion of the sample. As can be observed in the registered temperature profiles depicted in Fig. 3a, temperature gradients are developed, with higher temperature at the bottom because the combustion takes place in the expansion (lowest section) of the reactor.

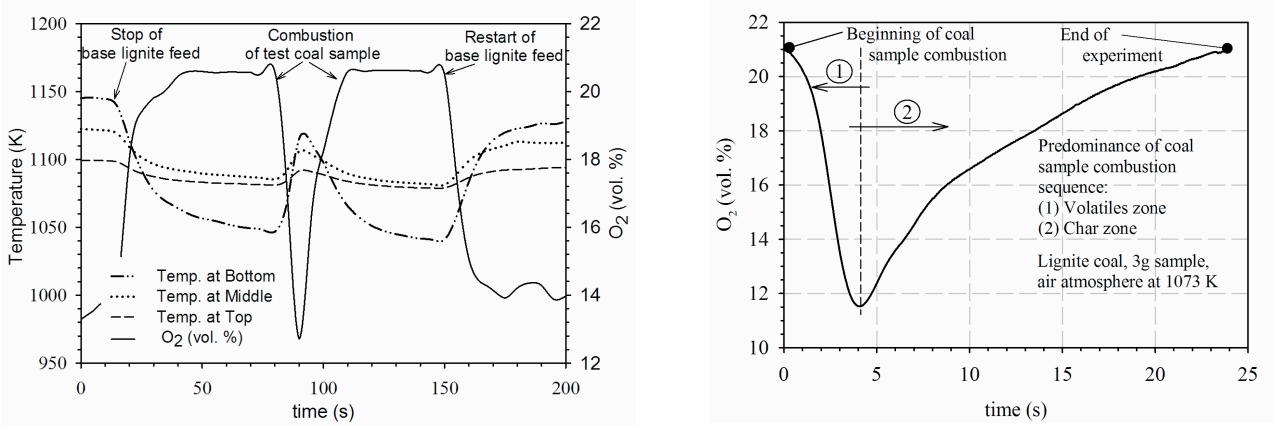

(a) (b)

Figure 3. Temperature and oxygen concentration curves of a typical test (a) and coal sample combustion sequence (b).

In the present study, trials are performed with Lusatian pre-dried lignite coal with 6.5% of ash in dry mass basis, and 57.9% volatile matter and 42.1% fixed carbon in daf basis with proximate analysis. Combustion of the samples, sieved to a size range of 1.250-2.000 mm, is carried out under air-fired and oxy-fired conditions. The fundamental approach for all experiments conducted is to keep baseline air-firing tests comparable to those performed under oxy-fuel conditions as similar as possible. In order to keep similar velocities within the combustion reactor the volumetric flow of the oxidizer is kept approximately constant for all experimental cases. Additionally, the reactor temperatures monitored by K-type thermocouples installed within the furnace are kept constant at three different levels (1073, 1173 and 1273 K). The average of the temperatures measured at the bottom, at the middle and the top of the reactor determines the gas reactor temperature levels to run the tests. In the reactor inlet, the oxygen molar fraction is 0.21.

The reactor operating conditions are summarized in the Table 1. It is important to mention that in the present study only the primary oxidizer inlet was utilized. In order to test the repeatability of the experimental data, experiments have been carried out with average of two to three replicates. The volumetric flow rate of oxidizer shown in Table 1 is taken in the reactor inlet at 900 K. The oxy-fuel atmosphere is composed by 21/79 (O_2/CO_2 vol. %).

Table 1. Experimental parameters for air-firing and oxy-fuel

Experimental condition	Air-firing	Oxy-fuel
O_2 in oxidizer (vol. %)	21	21
Oxidizer volume flow (m^3/h) at 900 K	23	26
Oxidizer temperature (K)	873	873
Gas reactor temperature (K)	1073 , 1173 , 1273	
Sample weight (g)	1	

5. GLOBAL KINETIC FORMULATION

The formulation is based on the oxygen concentration registered by the solid electrolyte oxygen sensor, as detailed in perspective and schematic views showed in Fig. 4, during the combustion of coal sample. Several studies in the last decades applied solid electrolyte sensors on the basis of stabilized zirconia for investigation of combustion processes in situ (Schotte et al., 2003; Lorentz and Rau, 1998; Stenberg et al., 1998). The main advantage of these sensors is their high sensitivity coupled with short response times (Shin et al., 2004; Badwal et al., 1988). In this research, a robust sensor for operating range temperature from 923 to 1723 K and able to endure the extreme conditions such as within furnaces is applied. According to the manufacturer of this sensor, the response time is between 8 and 15 milliseconds and the measure accuracy of oxygen concentration at atmospheric pressure has a relative error lower than 5%. This sensor uses a ceramic tube constructed with an oxygen ion conduction material of yttria stabilized zirconia (YSZ).

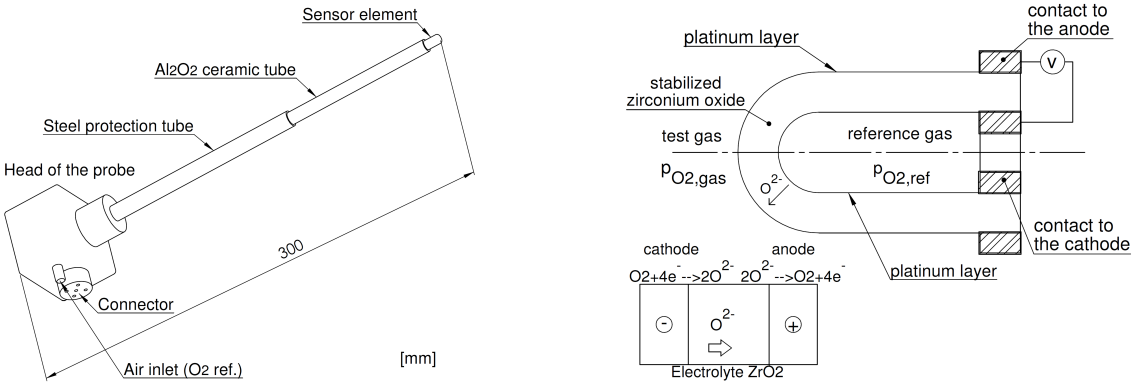

(a) (b)

Figure 4. Perspective view of the solid electrolyte oxygen probe (a) and a schematic drawing of the sensor element(b).

The output of this potentiometric sensor is a combined effect of chemical and electrical processes, which can be correlated by using thermodynamic equilibrium and fast kinetic reactions based on Nernst equation (Singhal and Kendall, 2003; Bhoga and Singh, 2007). The Nernst equation correlates the Gibb's free energy and electromotive force of a chemical system. For a solid electrolyte cell with two oxygen electrodes, the cell reaction is merely the transfer of oxygen from the higher to lower partial pressure, as detailed in Fig. 4b. The cell potential and oxygen partial pressures between the two electrodes (the reference electrode immersed in dry air, i.e. 21% O_2 vol., and the electrode immersed in gas combustion reactor) are related by the Nernst Equation (1).

$$U = \left(RT/\dot{n}_{el}F\right)\cdot \ln\left(p_{O_2,ref}/p_{O_2,gas}\right) \quad (1)$$

Substituting the oxygen partial pressures by molar fractions in Eq. (1) and rearranging it, the oxygen molar fraction of sampled gas can be calculated, knowing the cell potential and gas combustion temperature, according to Eq. (2).

$$f_{O_2,gas} = f_{O_2,ref} \exp\left(-4FU/RT\right) \tag{2}$$

The conservation of mass equation is applied to a control volume comprehending the whole combustion chamber. The oxygen molar flow rate consumed during the combustion of a sample can be expressed in terms of the temperature, oxygen molar fraction and pressure, assuming a volumetric flow rate and temperature within the reactor as reference, by following the ideal gas law relationships. The amount of oxygen consumed during the combustion reaction of a sample is calculated with the Eq. (3), by integrating the area above the oxygen molar fraction curve, at reactor outlet, Fig. 3b.

$$N_{O_2,cons} = \left(P_{atm}\dot{V}/RT\right)\cdot\int_0^t\left(f_{O_2,in} - f_{O_2,out}\right)dt \tag{3}$$

The equation to describe the rate of the oxygen consumed during the combustion of a sample is expressed in terms of the oxygen conversion and initial oxygen concentration by the Eq. (4).

$$\left(-r_{O_2}\right) = -C_{O_2,0}\, dX_{O_2}/dt \tag{4}$$

The oxygen conversion equation is calculated by knowing the moles of oxygen consumed until a specific time, divided by total of moles of oxygen consumed until the end of the combustion, as shown in Eq. (5).

$$X_{O_2} = N_{O_2,cons}/N_{O_2,tot} \tag{5}$$

The integral method of analysis is utilized to calculate the global kinetic parameters of the sample combustion, i.e. the order of reaction and the reaction rate constant (Levenspiel, 1999). Here, the coal combustion reaction rate is approximated by an unimolecular irreversible reaction according to Eq. (6).

$$\left(-r_{O_2}\right) = k_{eff}\; C_{O_2,0}^{n}\left(1 - X_{O_2}\right)^n \tag{6}$$

As the combustion of solids is characterized by heterogeneous reactions, an effective reaction rate constant is introduced in Eq. (7) in order to represent both the phenomena of mass transfer and chemical reaction kinetics (Lorentz and Rau, 1998). By combining the Eq. (4) and Eq. (6) and reorganizing the terms before integrating them, the following expression is obtained.

$$dX_{O_2}/(1 - X_{O_2})^n = -k_{eff.}\, C_{O_2,0}^{(n-1)}\, dt \tag{7}$$

The reaction order and effective constant rate are obtained according to literature (Levenspiel, 1999). The order of reaction is fixed when the best coefficient of determination (R^2) to fit the constant reaction rate is achieved.

The best fit, i.e. R^2=0.99, for the experiments is achieved with reaction order 1.0 for oxygen molar conversion with an interval between 0.2 and 0.9. Integrating the Eq. (7), the resulting expression is described by Eq. (8).

$$Ln\left(1 - X_{O_2}\right) = -k_{eff}\, t \tag{8}$$

6. RESULTS AND DISCUSSION

The behavior of O_2 concentration during the combustion of samples under air-fired and oxy-fired conditions for three temperature levels is plotted in Fig. 5. The resulting curves are oxygen concentration average values calculated for two samples at each time step of 0.05 s recorded by oxygen sensor along the curve. As shown in Fig. 5, differences in oxygen concentration values are observed under oxy-fired atmospheres at 1173 and 1273 K, compared with air-fired conditions. Figures 6 and 7 show photos taken from combustion samples videos under air-fired and oxy-fuel conditions at 1173 K with the camera focus on the reactor cone section. These photos are arranged in combustion sequence order, identified by capital letters A, B, C and D, with the aim to show the combustion main stages, as seen during the experiments, and to complement the oxygen concentration curves analysis. As shown in photo (A) for both atmospheres, the volatiles combustion is characterized by high luminosity flame, followed by char particles combustion, as shown in photos (B), (C) and (D). This is a typical combustion sequence of photos seen during the experiments at three temperature levels, nevertheless, at 1273 K, it's noteworthy comment that the char zone extension decrease and

mostly char particles are consumed together within the volatiles zone, resulting in higher oxygen concentration variations and lesser char particles burning at char zone than at lower temperatures (1073 and 1173K).

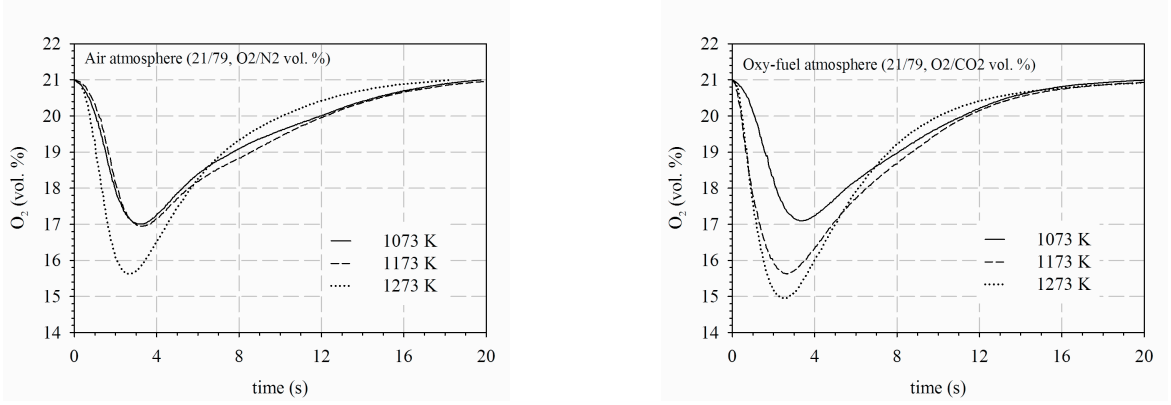

(a) (b)

Figure 5. Oxygen concentration curves under air-firing (a) and oxy-fuel with 21 vol.% O_2 (b).

As seen in Fig. 5 and the photos of Fig. 6 and 7, the total combustion times recorded by oxygen sensor are at about 20 s for both atmospheres and at the three levels of gas temperature. This is due to the oxygen sensor stabilization stage (from 20.5% O_2 vol.) and the predominance of advective terms of oxygen transport equation.

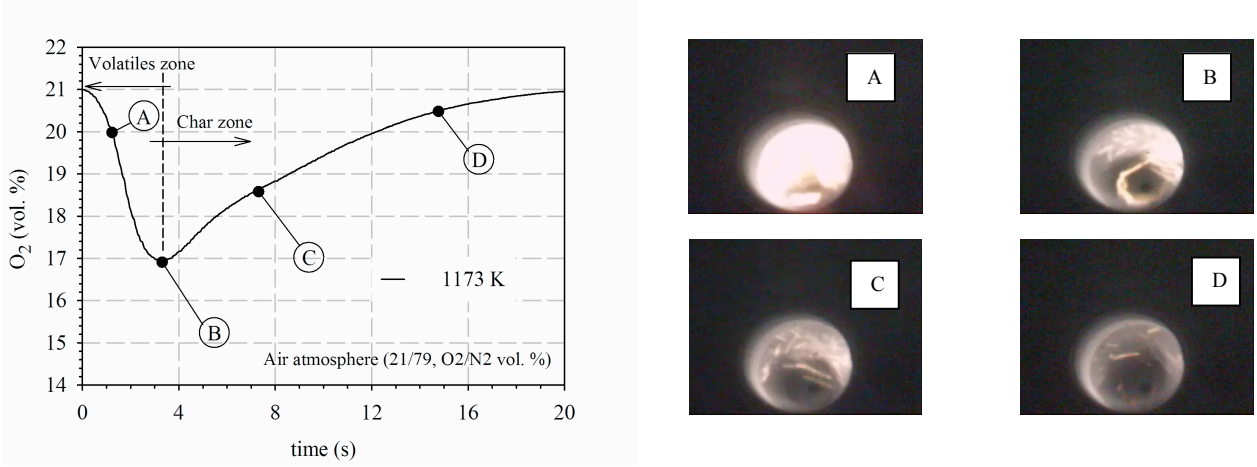

(a) (b)

Figure 6. Oxygen concentration curve under air atmosphere (a) and photos of the sample combustion sequence (b).

As seen in the photos of Fig. 6 and 7, most of char particles at stage (D) are almost complete burned and lesser particles are visible in the video than other stages (B, C), indicating the combustion reaction rate is due to complete, and the advective terms of the oxygen transport equation are influencing the oxygen sensor concentration measurements. This effect is more evident at 1273 K, where most of the char combustion particles are already burned at stage (D).

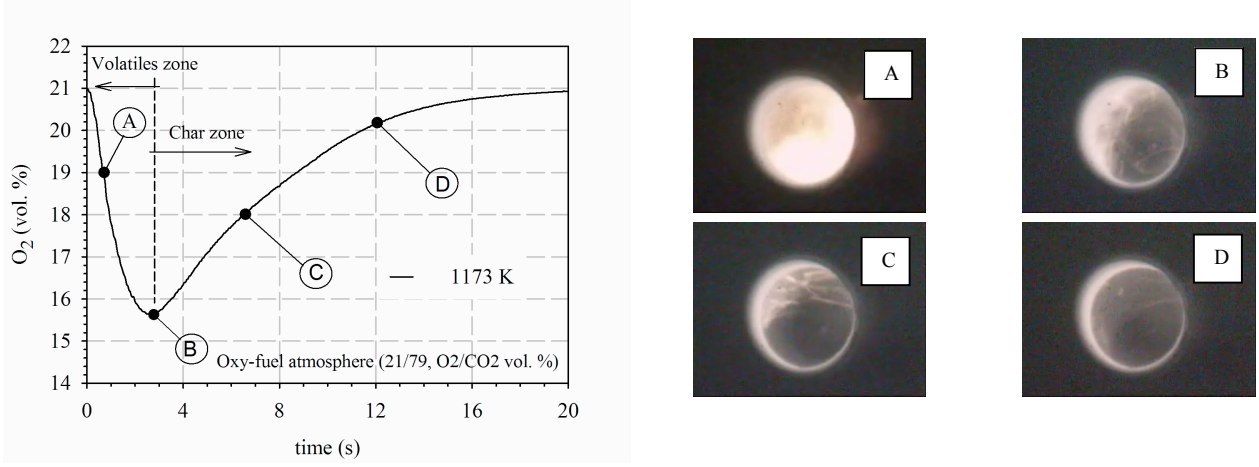

(a) (b)

Figure 7. Oxygen concentration curve under oxy-fuel atmosphere (a) and photos of the sample combustion sequence(b).

In order to estimate the Lignite reactivity based on the oxygen concentration curves plotted, the following sequence of graphs depicted in Fig. 8 are required and illustrate the calculation, by applying the fundamental equations of item 5 for air-fired and oxy-fuel conditions, assuming that combustion reaction rate is proportional to the oxygen rate consumed by coal sample. For example, the Fig. 8a shows the oxygen concentration curve obtained at 1073 K under air-fired conditions, and from this curve all other variables are determined and plotted, as oxygen consumption, oxygen conversion and finally the effective constant reaction rate, showed in Fig. 8b, 8c and 8d respectively.

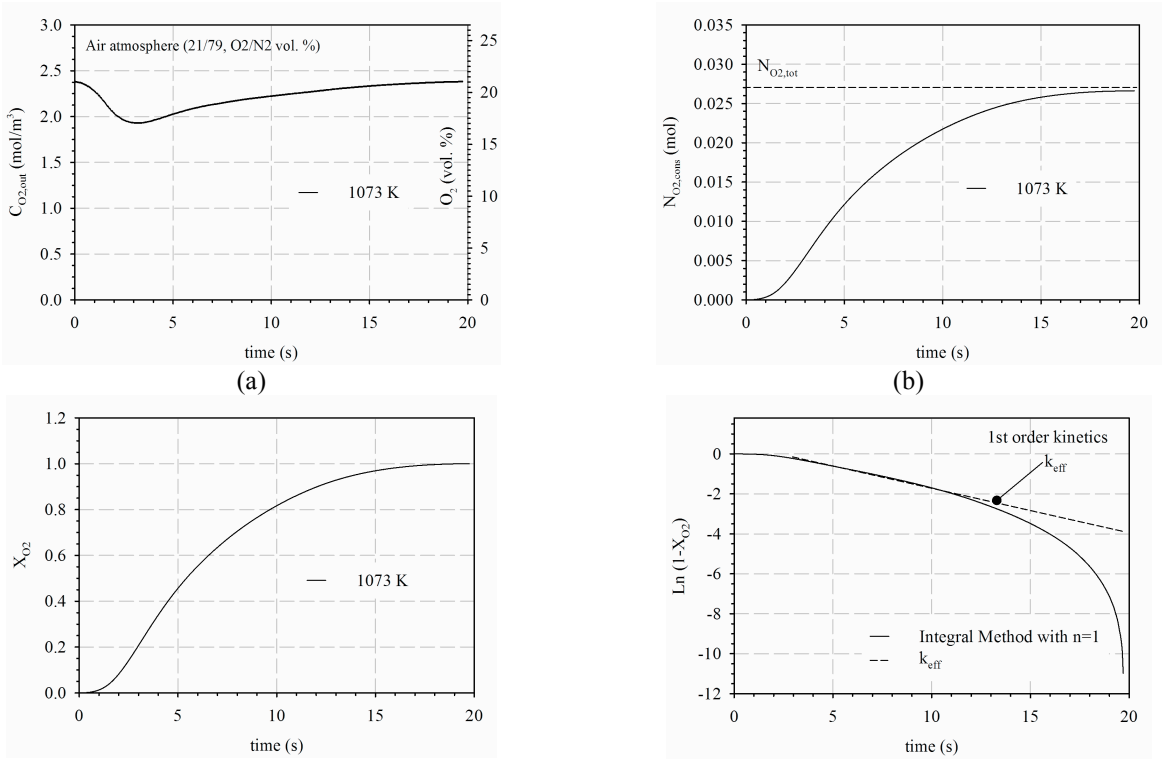

Figure 8. Oxygen concentration curve (a), oxygen consumption (b), oxygen conversion (c) and k_{eff} fitting (d).

The Fig. 9 shows the effective constant reaction rate values under air-fired and oxy-fuel conditions at each temperature level determined from the linear least-squares fitting method, as illustrated in Fig. 8d. The best fitting interval obtained to calculate the constant reaction rate is between 0.2 and 0.9 of oxygen conversion, comprehending the char zone predominantly, where the constant reaction rate is constant.

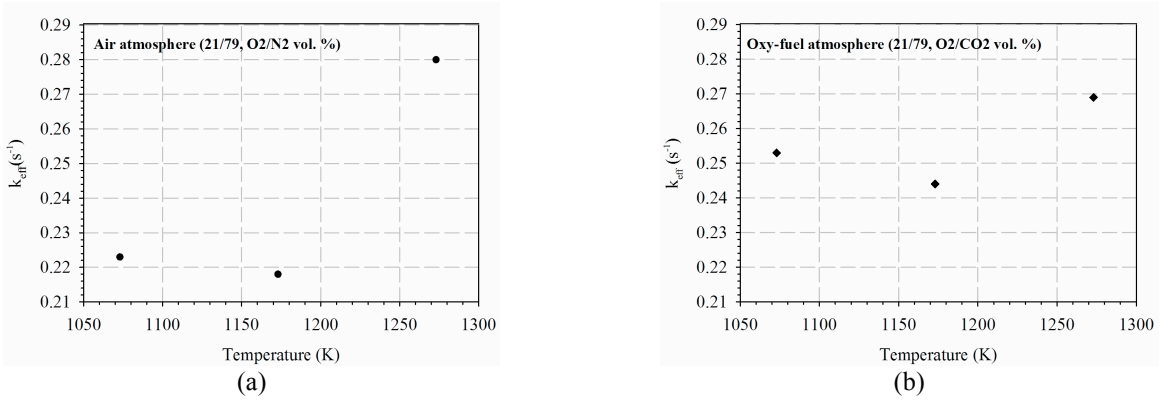

Figure 9. Effective constant reaction rate values for air atmosphere (a) and oxy-fuel atmosphere (b)

As seen in Fig. 9b, under oxy-fuel conditions are obtained higher constant reaction rate values than air-fired conditions at 1073 and 1173 K. These results may indicate the influence of gasification reaction due to higher partial pressure of CO_2 ($C + CO_2 \leftrightarrow 2CO$). This reaction is heavily affected by temperature, increasing its reaction rates from 1073 K as verified previously by other authors utilizing other experimental methods (Hecht et al., 2011; Zhang et al., 2010a; Rathnam et al., 2009). At 1273 K, the effective constant reaction rate values are close to each other at both atmospheres, which may indicate that the gasification reaction has not more influence. However, as the present study is

a global method to determine the fuel reactivity, represented by the effective constant reaction rate values, more investigation is required to segregate the influence of the advective terms on the combustion char reaction rate and apply a suitable particle coal combustion model to determine the rate controlling phenomena on the coal combustion reaction. This investigation can contribute to understand the whole phenomena, which is complex, and may elucidate the reason why the oxygen concentration curves under air-fired conditions at 1073 and 1173 K have the same behavior.

7. CONCLUSIONS

This work is aimed at a fundamental study of the kinetics of combustion of one pre-dried lignite coal under air-fired and oxy-fired conditions. The research is based on experimental activities carried out in a laboratory cyclone reactor. The overall combustion kinetics is followed by the measurements of O_2 concentration and temperature within the furnace and oxidizer flow rates. Higher effective reaction rate constant values are obtained under oxy-fuel than air-firing conditions at 1073 and 1173 K. However, it's early to affirm that these results are due only to the gasification reaction of CO_2, since to assure this phenomena is required the incorporation of a suitable char combustion model, as for example, a shrinking core model, contemplating the gasification reaction of CO_2, and what is the rate controlling phenomena (chemical reaction and/or mass transfer diffusion rates), and the segregation of advective terms of oxygen transport equation influence on the combustion char reaction term. With respect to the linearization method applied to obtain the effective reaction rate constants, the reaction order of 1.0 and interval of oxygen conversion between 0.2 and 0.9 provides a representative effective reaction rate constant of the combustion process at 1073 and 1173 K for the char, where the effects of advective terms of oxygen transport equation at the char zone are reduced due to the presence of more particles burning and consuming oxygen, as observed in the photos and the oxygen concentrations curves.

8. REFERENCES

Badwal, S.P.S., Bannister, M,J. and Chiacci F.T., 1988. "Response rate techniques for zirconia-based Nernstian oxygen sensors". Journal of Applied Electrochemistry, Vol. 18, No. 4, pp. 608-613.

Bhoga, S. S., Singh, K., 2007. "Electrochemical solid state gas sensors: review". Ionics, Vol.13, No. 6, pp. 417-427.

Brix, J., Jensen, P.A., Jensen, A.D., 2010. "Coal devolatilization and char conversion under suspension fired conditions in O_2/N_2 and O_2/CO_2 atmospheres". Fuel, Vol. 89, No. 11, pp. 3373-3380.

Hecht, E.S., Shaddix, C.R., Molina, A., Haynes, B.S., 2011. "Effect of CO_2 gasification reaction on oxy-combustion of pulverized coal char". Proceedings of Combustion Institute, Vol. 33, No. 2, pp. 1699-1706.

Levenspiel, O., 1999. "Chemical Reaction Engineering". 3rd Edition, John Wiley & Sons, New York, USA.

Liu, H., 2009. "Combustion of coal chars in O_2/CO_2 and O_2/N_2 mixtures: a comparative study with non-isothermal thermogravimetric analyzer (TGA) tests". Energy and Fuels, Vol. 23, No. 9, pp. 4278-4285.

Lorentz, H., Rau, H., 1998. "A new method for investigating the combustion behavior of solid fuel in FBC". Fuel, Vol. 77, No. 3, pp. 127-134.

Rathnam, R.K., Elliot, L.K., Wall, T., Liu, Y., Moghtaderi, B., 2009. "Differences in reactivity of pulverized coal in air (O_2/N_2) and oxy-fuel (O_2/CO_2) conditions". Fuel Processing Technology, Vol. 90, No. 6, pp. 797-802.

Schotte, E., Lorenz, H., Rau H., 2003. "Investigating gasification process of solid fuels by in situ gas potentiometric oxygen probes". Chemical Engineering Technology, Vol. 26, No. 7, pp. 774-778.

Shin, W., Izu, N., Matsubara, I., Murayama, N., 2004. "Millisecond-order response measurement for fast oxygen gas sensors". Sensors and Actuators B: Chemical, Vol. 100, No. 3, pp. 395-400.

Singhal, S.C. and Kendall, K., 2003. "High Temperature Solid Oxide Fuel Cells: Fundamentals, Design and Applications". Elsevier Ltda, Oxford, UK.

Stenberg, J., Amand, L.E., Hernberg, R., Leckner, B., 1998. "Measurements of gas concentrations in a fluidized bed combustor using laser-induced photoacoustic spectroscopy and zirconia cell probes". Combustion and Flame, Vol. 113, No. 4, pp. 477-486.

Tappe, S., Krautz, H.J., 2009. "ALVA 20: A 20 kWth Atmospheric Laboratory Test Facility to Investigate the Combustion Behaviour under Close-to-Reality Conditions". Proceedings of the European Combustion Meeting, pp. 6.

Toftegaard, M. B., Brix, J., Jensen, P.A., Glarborg, P., Jensen, A.D., 2010. "Oxy-fuel combustion of solids fuels". Progress in Energy and Combustion Science, Vol. 36, No. 5, pp. 585-625.

Zhang, L., Binner, E., Chen, L., Qiao, Y., Li, C., Bhattacharya, S., Ninomiya, Y., 2010a. "Experimental investigation of the combustion of bituminous coal in air and O_2/CO_2 mixtures: 1. Particle imaging of the combustion of coal and char". Energy Fuels, Vol. 24, No. 9, pp. 4803-4811.

Zhang, L., Binner, E., Chen, L., Qiao, Y., Li, C., 2010b. "In situ diagnostics of Victorian brown coal combustion in O_2/N_2 and O_2/CO_2 mixtures in drop-tube furnace". Fuel, Vol. 89, No. 10, pp. 2703-2712.

9. RESPONSIBILITY NOTICE

The authors are the only responsible for the printed material included in this paper.